

Time Reversal for Damage Detection in Pipes

Yujie Ying^{a*}, Joel Harley^b, James H. Garrett, Jr.^a, Yuanwei Jin^c, José M.F. Moura^b, Nicholas O'Donoghue^b, Irving J. Oppenheim^a, and Lucio Soibelman^a

^aDept. of Civil and Environmental Engineering, Carnegie Mellon University, Pittsburgh, PA 15213

^bDept. of Electrical and Computer Engineering, Carnegie Mellon University, Pittsburgh, PA 15213

^cDept. of Engineering and Aviation Sciences, University of Maryland Eastern Shore, Princess Anne, MD 21853

ABSTRACT

Monitoring the structural integrity of vast natural gas pipeline networks requires continuous and economical inspection technology. Current approaches for inspecting buried pipelines require periodic excavation of sections of pipe to assess only a couple of hundred meters at a time. These inspection systems for pipelines are temporary and expensive. We propose to use guided-wave ultrasonics with Time Reversal techniques to develop an active sensing and continuous monitoring system.

Pipe environments are complex due to the presence of multiple modes and high dispersion. These are treated as adverse effects by most conventional ultrasonic techniques. However, Time Reversal takes advantage of the multi-modal and dispersive behaviors to improve the spatial and temporal wave focusing. In this paper, Time Reversal process is mathematically described and experimentally demonstrated through six laboratory experiments, providing comprehensive and promising results on guided wave focusing in a pipe with/without welded joint, with/without internal pressure, and detection of three defects: lateral, longitudinal and corrosion-like. The experimental results show that Time Reversal can effectively compensate for multiple modes and dispersion in pipes, resulting in an enhanced signal-to-noise ratio and effective damage detection ability. As a consequence, Time Reversal shows benefits in long-distance and low-power pipeline monitoring, as well as potential for applications in other infrastructures.

Keywords: Time Reversal, guided waves, damage detection, pipeline, ultrasonics, Structural Health Monitoring (SHM), and Nondestructive Evaluation (NDE).

1. INTRODUCTION

Ultrasonic guided wave technology has provided a useful tool for Structural Health Monitoring (SHM) and Nondestructive Evaluation (NDE) applications over decades. Guided waves are sensitive to surface and internal damage in structures and are able to propagate over long distances¹⁻³. However, guided wave propagation in pipes is complicated due to the presence of multiple modes at each frequency and its dispersion characteristics^{3,4}. Current pipeline inspection approaches often choose narrowband and low frequency excitation to selectively exploit a single mode for inspection, so as to suppress unwanted modes and to reduce the dispersive effects^{5,6}. Those conventional approaches usually involve periodic excavation of a section of pipe and attachment of large rings of transducers. The systems are temporary, bulky and require high transmission powers to inspect over long distances. Therefore, the technology and process is very expensive and not efficient for guided wave propagation in a pipe.

Time Reversal is a signal processing technique to increase the spatial and temporal wave focusing⁷. Time Reversal techniques have been exploited for Lamb waves in thin plates, leading to an enhanced signal level and compensation for multiple modes and dispersion⁸⁻¹¹. Previous research has also shown Time Reversal focusing is beneficial from highly dispersive environment^{8,12-14}. Therefore, we have developed Time Reversal focusing technique for the complex pipe environment by taking advantage of the multimodal, dispersive guided waves in pipes.

* Contact author: yying@cmu.edu.

In this paper, we first briefly present the characteristics of guided waves in pipes, followed by a mathematical description of the Time Reversal focusing process. We then provide comprehensive laboratory test results to examine Time Reversal's applications to focus ultrasonic waves in pipes, and to demonstrate the capability of Time Reversal change focusing to illuminate different types of defects.

2. GUIDED WAVES IN PIPES

Guided waves are ultrasonic waves propagating through a medium with geometric boundaries⁴. The boundaries form a waveguide such as a plate, rod, or pipe. Guided waves are multi-modal and dispersive in nature: multiple wave modes can be generated at different frequencies; dispersion is the phenomenon that the velocity of different modes depends on the frequency.

Guided waves in pipes or hollow cylinders contain three fundamental classes of wave modes, i.e. an infinite number of longitudinal modes, an infinite number of torsional modes, and a doubly infinite number of flexural modes. Longitudinal modes and torsional modes are axisymmetric, while flexural modes are non-axisymmetric¹⁵. We use two indices M and N to denote the fields of the guided wave modes. The index N, named circumferential order, gives the order of symmetry around the axes of the cylinder, so that for axisymmetric modes, N equals 0; the index M, named family order, sorts the modes for a given family. Therefore, longitudinal modes, torsional modes, and flexural modes are often written as L (0, M), T (0, M) and F (N, M)¹⁶.

In a cylindrical coordinate system of a pipe, $\mathbf{x} = (r; \theta; z)$, we define $r(\mathbf{x}, t)$ as the superposition of each mode at a given location \mathbf{x} at a given time t, obtained from¹⁷

$$r(\mathbf{x}, t) = \sum_{M=0}^{\infty} a_M e^{j(\omega t - \beta_M z)} + \sum_{N=0}^{\infty} \sum_{M=0}^{\infty} a_M^N e^{j(\omega t - \beta_M^N z)} \quad (1)$$

where ω is the angular frequency, a_M^N and β_M^N are the amplitude and wave number due to the Mth mode of the Nth family, respectively, and denoted as a_M and β_M when N=0, i.e. for axisymmetric modes.

Note that $r(\mathbf{x}, t)$ is also a received response produced by an excitation $s(t)$, i.e. the different guided wave modes are excited by $s(t)$. Therefore, in the frequency domain, the input excitation and the response are related through a pipe transfer function $H(\mathbf{x}, \omega)$, as expressed in the following:

$$R(\mathbf{x}, \omega) = S(\omega) H(\mathbf{x}, \omega) \quad (2)$$

where $R(\mathbf{x}, \omega)$ and $S(\omega)$ are the Fourier Transform of $r(\mathbf{x}, t)$ and $s(t)$, respectively.

3. TIME REVERSAL FOCUSING

In Time Reversal processing, we assume the waveguide is reciprocal and stationary⁷. Reciprocity ensures the same signals are received when the waves propagate backward; stationary means the results do not vary over time. Section 3.1 and 3.2 mathematically describe the Time Reversal process of guided waves in a pipe.

3.1 Time Reversal focusing of guided waves

We consider performing pitch-catch method using two in-line transducers attached on the surface a pipe, one as a transmitter and the other as a receiver, so that Eq.(2) can be simplified as¹⁷⁻¹⁹

$$R(\omega) = S(\omega) H(\omega) \quad (3)$$

The received signal is then time-reversed and energy-normalized, before travelling back through the pipe. We note that in the frequency domain, time reversal is equivalent to the negation of angular frequency ω , thus the time-reversed and energy-normalized signal becomes

$$S^{TR}(\omega) = kR(-\omega) = kS(-\omega)H(-\omega) \quad (4)$$

where k is the energy normalization term, ensuring the time reversed signal has the same energy as the original input, expressed as

$$k = \sqrt{\frac{\int_{-\infty}^{\infty} |S(\omega)|^2 d\omega}{\int_{-\infty}^{\infty} |R(\omega)|^2 d\omega}}. \quad (5)$$

When the new input signal is transmitted back through the pipe, the received signal can now be written as

$$\begin{aligned} Y(\omega) &= S^{TR}(\omega)H(\omega) \\ &= kS(-\omega)H(-\omega)H(\omega) \end{aligned} \quad (6)$$

If we assume that phase velocity $v_m(\omega)$ is even symmetric with respect to ω such that $v_m(\omega) = v_m(-\omega)$, then

$$\beta_M^N(-\omega) = \frac{-\omega}{v_m(-\omega)} = -\frac{\omega}{v_m(\omega)} = -\beta_M^N(\omega). \quad (7)$$

Therefore, we have $R(-\omega) = R^*(\omega)$. Since $S(-\omega) = S^*(\omega)$ due to the conjugate symmetric Fourier Transform of the driven signal $S(\omega)$, it results in

$$H(-\omega) = H^*(\omega) \quad (8)$$

Therefore, Eq. (6) can be rewritten as

$$\begin{aligned} Y(\omega) &= kS^*(\omega)H^*(\omega)H(\omega) \\ &= kS^*(\omega)|H(\omega)|^2 \end{aligned} \quad (9)$$

Eq. (9) shows the received signal has the same phase-profile as the conjugate or time-reversed excitation signal. This is an indication of a large reduction in dispersion and multi-modal effects after Time Reversal is applied. The guided wave modes focus at the original source at a single point in time, leading to an enhanced signal level and compensation for multiple modes and dispersion in pipe environment. As a result, we expect the time domain signal to be symmetric with a large peak at the center.

3.2 Time Reversal change focusing

The above section has shown Time Reversal leads to focusing of various guided wave modes at the original source. Here, we describe a similar Time Reversal process, but for focusing at “changes” caused by damage in a pipe. The basic idea is to obtain the response component due to the changes by background subtraction and then time-reverse and retransmit the response due to the changes through the pipe. Those changes are also focused, Time Reversal change focusing. In other words, the presence of damage can be present as a significant peak at the center of the Time Reversal focused signal.

We assume we are able to measure the response of the pipe before any damage occurs and this response is stationary over time, thus the received response due to the background “clutter” is given by¹⁸

$$R_C(\omega) = S(\omega)H_C(\omega). \quad (10)$$

$S(\omega)$ is known, and $R_C(\omega)$ can be measured, so Eq.(10) gives $H_C(\omega)$, the clutter transfer function.

When the damage is induced, the received signal becomes

$$R(\omega) = S(\omega)H(\omega) = S(\omega)(H_C(\omega) + H_T(\omega)). \quad (11)$$

where $H_T(\omega)$ is the transfer function of the “target” referring to damage or “change” in the pipe.

The response due to the “target” is the difference between the received signal and the response due to the “clutter”, therefore

$$\begin{aligned} R_T(\omega) &= R(\omega) - R_C(\omega) \\ &= S(\omega)H_T(\omega) \end{aligned} \quad (12)$$

We then time-reverse and energy-normalize the response due to the “target” or the “change” in the pipe, and obtain a new excitation which will be sent backward through the pipe. This time-reversed and energy-normalized signal can be expressed as

$$\begin{aligned} S_T^{TR}(\omega) &= kR_T(-\omega) \\ &= kS(-\omega)H_T(-\omega) \\ &= kS^*(\omega)H_T^*(\omega) \end{aligned} \quad (13)$$

where k is the energy normalization term given by Eq. (5).

When the new input signal is transmitted back in the pipe, the received signal is

$$\begin{aligned} Y(\omega) &= S_T^{TR}(\omega)H(\omega) \\ &= kS^*(\omega)H_T^*(\omega)(H_C(\omega) + H_T(\omega)) \\ &= kR_T^*(\omega)H_C(\omega) + kS^*(\omega)|H_T(\omega)|^2 \end{aligned} \quad (14)$$

After Time Reversal process, this received signal also consists of two components, the response due to the “clutter” and the response due to the “target”. The “clutter” response can be determined, since $H_C(\omega)$ is known from Eq. (10) and $R_T(\omega)$ is measured according to Eq. (12). As a result, we subtract the “clutter” component from Eq.(14) and obtain the equation of the change in the pipe as

$$\begin{aligned} Y_T(\omega) &= Y(\omega) - kR_T^*(\omega)H_C(\omega) \\ &= kS^*(\omega)|H_T(\omega)|^2 \end{aligned} \quad (15)$$

We can see Eq. (15) is similar to Eq.(9), but the focused signal is now caused by damage in the pipe. We expect to see a large peak at the center of the time domain signal as an indication of the defects' existence. Therefore, Time Reversal change focusing provides an easy-implemented metric for damage detection in a pipe, without any interpretation of wave modes as done by many conventional methods.

4. EXPERIMENTAL RESULTS

In this section, we present experimental results of Time Reversal focusing technique applied to six different laboratory scenarios. The first three subsections discuss Time Reversal focusing of guided waves in a pipe with/without welded joint, with/without internal pressure; the next three demonstrate Time Reversal change focusing for detection of three different defects: lateral, longitudinal and corrosion-like.

All the experiments were conducted on steel pipe specimens with two piezoelectric wafer transducers (Lead Zirconate Titanate, PZT 5A4E) mounted on the surface of each pipe using cyanoacrylate adhesive. One PZT transducer functioned as a transmitter and the other as a receiver, performing in pitch-catch method. A National Instruments PXI system was used to drive the transmitter and to record waveforms at the receiver. A sinc pulse was chosen as the input signal (Figure 2a), because it resulted in more modes and more dispersion (as compared to narrowband excitation), which are beneficial for Time Reversal^{12,17}. Note that all the following Time Reversal focused signals were generated mathematically using the measured received responses by Eq. (9) or (15). The scheme of the experiments is shown in Figure 1. The specifications of the experimental specimens are given in Table 1. The experimental results are summarized in Table 2 and Table 3.

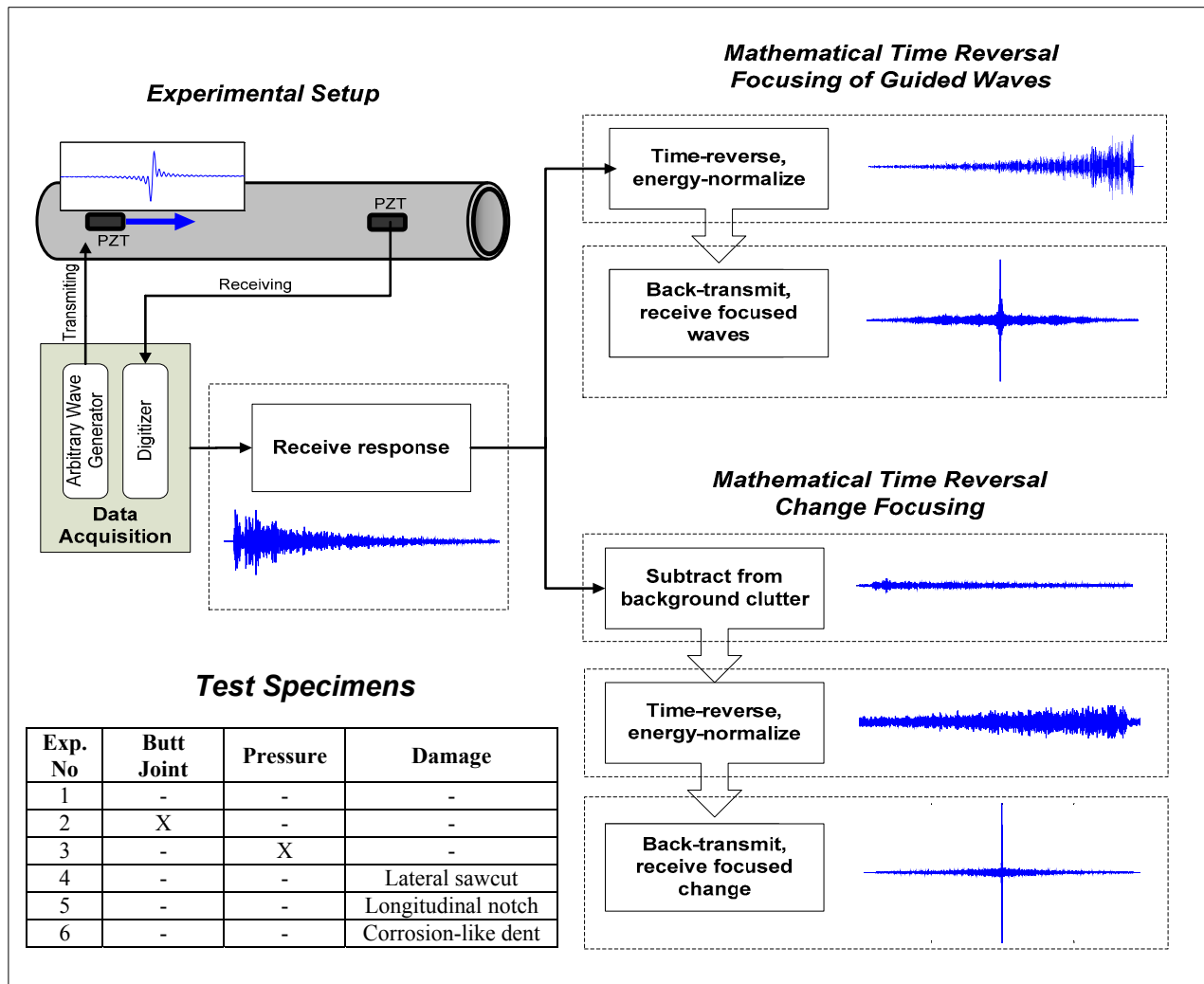


Figure 1. Scheme of the experiments.

Table 1. Specifications of the experimental specimens

Exp. No	Steel Pipe Specimens			Transducers		
	Dimensions [mm]			Specifications	Size [mm*mm]	Dist. ^c [mm]
	Length	OD ^a	WT ^b			
1	1833	70	4	-	20*8	1200
2	1833	70	4	10-mm-wide welded butt joint, 900 mm from one end of the pipe.	20*8	1200
3	1833	70	4	83.7 psi internal pressure.	20*8	1200
4	3050	60.3	3.6	Lateral sawcut: 1 mm wide, 1 mm deep and 25 mm in arc dimension, 590 mm from the transmitter.	10*5	3050
5	1730	74	5	Longitudinal defect: 220 mm long, 3 mm wide and 1 mm deep, 450 mm from the transmitter.	12*6	1000
6	1730	74	5	Corrosion-like defect: major axes 20 mm, minor axes 15 mm, 1 mm deep, 300 mm from the transmitter.	12*6	1000

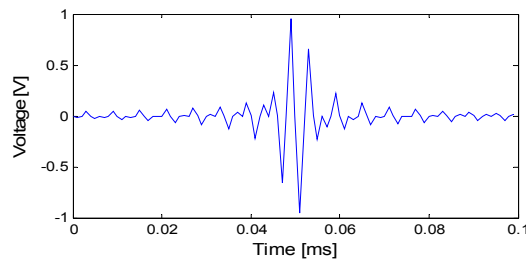
(^aOD: outside diameter; ^bWT: wall-thickness; ^cDist: distance between the transmitter and the receiver).

4.1 Guided waves focusing in a pipe

The experiment was performed on a pipe with length 1833 mm, outside diameter 70 mm and wall thickness 4 mm. Two PZT wafer transducers were located 1200 mm apart on the pipe. Each wafer was 20 mm long, and 8 mm wide.

When the transmitter is excited by a sinc pulse centered at 250 kHz shown in Figure 2a, the received response appears to contain a large amount of guided wave modes which are very complex and difficult to be separated or interpreted, as shown in Figure 2b. However, after performing the Time Reversal focusing process, different wave modes are compressed, presenting as a large peak at the center of the plot shown in Figure 2c. This peak is formed as a consequence of focusing wave modes as explained by Eq.(9). Moreover, we can see a significant increase in the maximum amplitude of the received signal, from 41.0 mV to 103.9 mV, an 8.1 dB increase after Time Reversal is applied.

The following experiments will discuss the effectiveness of Time Reversal focusing technique in some more complicated scenarios rather than in the seamless, non-pressurized and undamaged pipe that we used for this experiment.



(a)

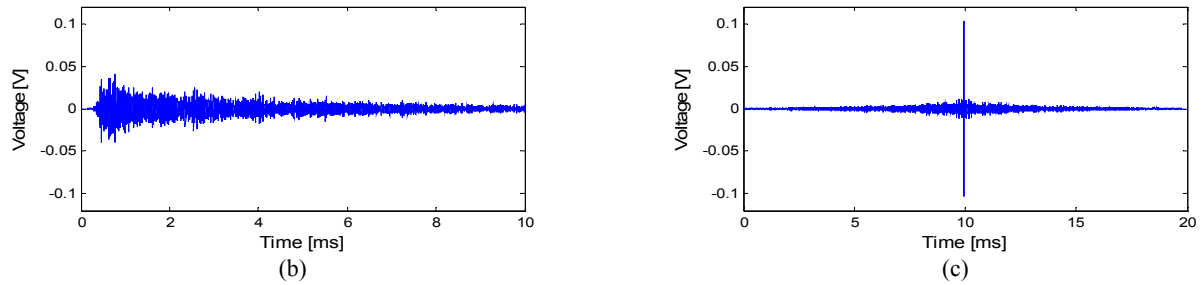


Figure 2. (a) 250 kHz sinc pulse excitation, (b) received signal, and (c) Time Reversal focused signal.

4.2 Pipe with a welded butt joint

The pipe specimen was nominally identical as the one we used in the previous experiment, but with a 10-mm-wide welded butt joint located 900 mm from one end of the pipe. The size and location of the two PZTs as well as the excitation signal, a 250 kHz sinc pulse shown in Figure 2a, were the same as with the jointless pipe.

We can see from Figure 3 a 6.2 dB increase in the maximum received amplitude, from 18.2 mV to 37.2 mV, after Time Reversal is applied. The experimental results in Figure 2 and Figure 3 show in parallel that Time Reversal can effectively compress waves temporally and spatially in both cases, with and without a welded butt joint. However, it is noted that the maximum received amplitude in the pipe with the welded butt joint is less, by 7.1 dB, than the amplitude compared with the strength of the received signals in the jointless pipe.

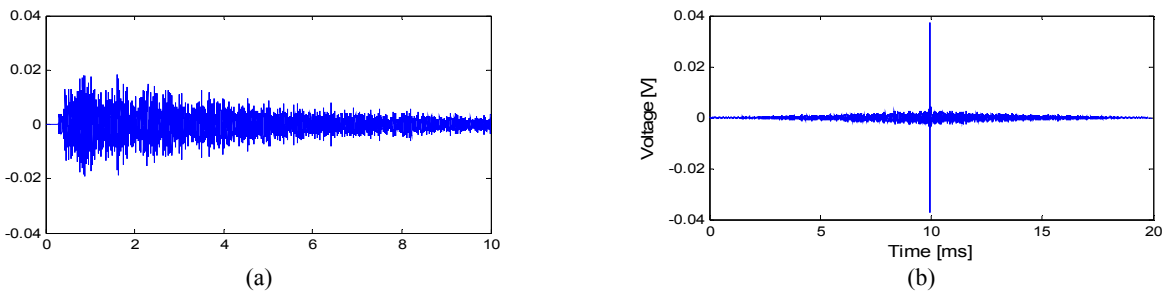


Figure 3. (a) Received signal, and (b) Time Reversal focused signal in the pipe with a welded butt joint.

We hypothesize that the welded butt joint reflects a significant portion of the ultrasonic waves, resulting in an energy loss in the pipe. To study the hypothesis we performed supplementary experiments on the pipe with a welded butt joint using a Krautkramer USPC 2100 system and angle beam/wedge transducers. Those transducers were sequentially positioned at different locations to capture guided wave behaviors along different paths in the pipe. The received signals were displayed in strip-chart format with an adjustable amplifier. To compare the strength of the signals, we fixed the maximum amplitudes at the same level and recorded the required gain (dB) of the amplifier, so that less gain indicated stronger signals. Figure 4 is a snapshot showing a received waveform in pulse-echo mode with a signal wedge transducer placed 300 mm from the welded butt joint. An evident echo is received at about 120 μ s, which is consistent with the path length 600 mm and the longitudinal wave velocity roughly 5 km/s. In pitch-catch method, Figure 5 shows a 10 dB energy loss when a welded butt joint is between two wedge transducers, compared to the received signal when the two transducers are located at different section of the pipe with no weld in between. These experimental results are consistent with the previous experiments performed with PZT wafers on two pipes, with/without a welded butt joint. We can safely conclude that welded joint causes a considerable portion of the waves to be reflected back from the weld without reaching the receiver.

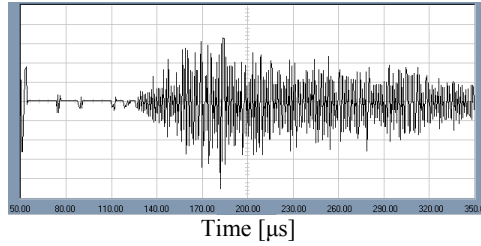


Figure 4. Pulse-echo method: reflection waves from the welded butt joint with gain 95.3 dB.

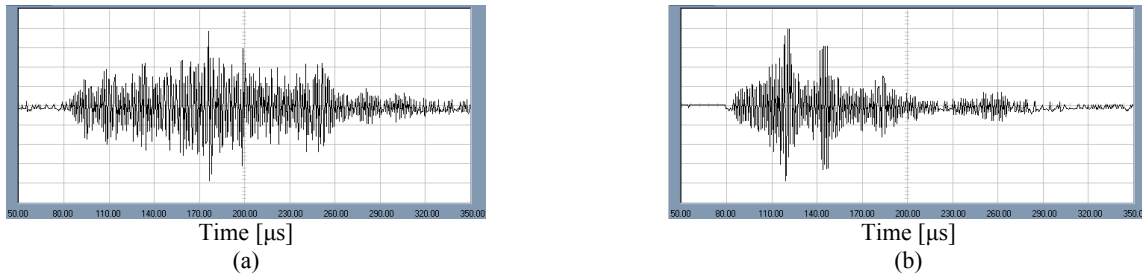


Figure 5. Pitch-catch method: received signals when (a) the joint is between the two transducers with gain 95.1 dB, and (b) no weld is in between with gain 85 dB.

Figure 4 and Figure 5 also show a pronounced waveform difference among reflection waves, transmission waves from the joint, and waves propagating without encountering the joint. The discrepancy indicates a large difference of the joint influence on different wave modes. This joint effect makes the wave modes even more difficult to be distinguished for some conventional detection methods that are based on mode selection and interpretation. However, Time Reversal provides an enhanced peak value despite the fact that the weld causes energy loss in the pipe. Moreover, the results are specific to the experimental configuration, and there exist several engineering choices to limit or overcome this effect, which is not discussed in this paper.

4.3 Pipe with internal pressure

The test specimen for this experiment has a welded-on cap and a pressure gauge at the two ends of the pipe to control the internal atmospheric pressure, with length 1833 mm, outer diameter 70 mm and wall thickness 4 mm. Two PZT wafers, sized at 20 mm x 8 mm, were mounted 1200 mm apart on the pipe. A sinc pulse centered at 250 kHz was chosen as the input signal (Figure 2a).

Similar to the experimental results in the pipe with a welded butt joint, Time Reversal presents a significant spatial and temporal focusing of guided waves in the pipe. Figure 6 shows Time Reversal amplifies the peak value of the received signal from 33.8 mV to 97.5 mV, a 9.2 dB increase, when the pipe is not pressurized. Figure 7 shows the maximum received amplitude increases from 23.2 mV to 33.7 mV, a difference of 3.3 dB, when the pipe is pressurized to 83.7 psi. It should be noted that the high air pressure inside the pipe not only affects the amplitude of the ultrasonic waves, leading to a 3.3 dB drop in the maximum received amplitude when the internal pressure is increased by 83.7 psi, but also restricts Time Reversal's ability of enhancing the peak level, jumping down to a 3.3 dB increase from a 9.2 dB augment.

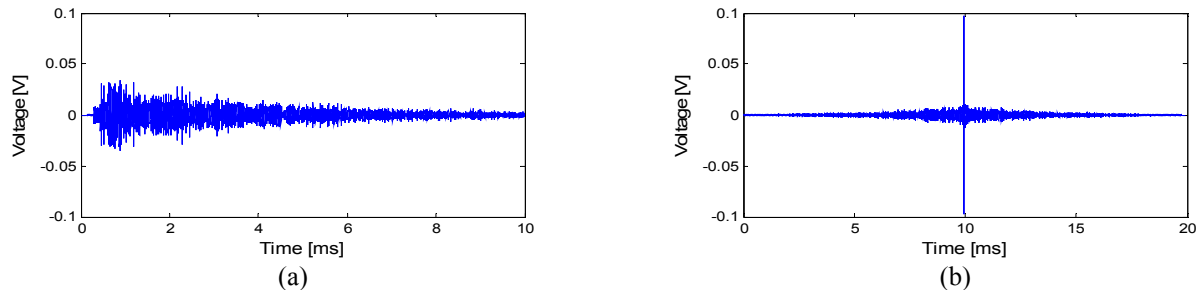


Figure 6. (a) Received signal, and (b) Time Reversal focused signal with 0 psi internal pressure.

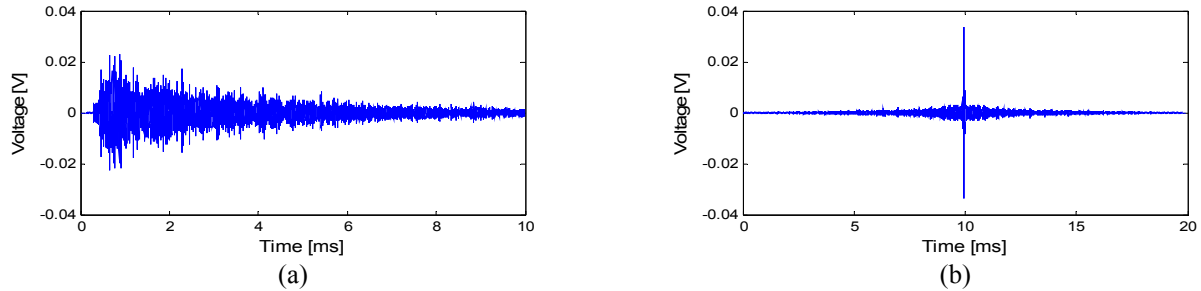


Figure 7. (a) Received signal, and (b) Time Reversal focused signal with 83.7 psi internal pressure.

4.4 Pipe with a lateral defect

This experiment was performed on a pipe specimen with length 3050 mm, outside diameter 60.3 mm and wall thickness 3.6 mm. A PZT wafer transmitter and receiver pair was mounted at the two ends of the pipe. Each wafer was 10 mm long and 5 mm wide. The transmitter was excited by a 200 kHz sinc pulse. We induced a small and partial-thickness sawcut at the lateral direction, 1 mm wide, 1 mm deep and 25 mm in arc dimension, 590 mm from one end of the pipe.

Figure 8(a)-(c) shows the received signals before and after the lateral cut was created; Figure 8(d) and (e) gives the changes of the responses after background subtraction. Those changes are very weak and indistinguishable. However, by performing Time Reversal change focusing on Figure 8(d) and (e), we obtain a very significant difference between these two cases, with and without the lateral defect present. As shown in Figure 9, the peak level of the change focused signal increases from 0.0037 mV to 0.1243 mV, a difference of nearly 34 times or 30.6 dB. The noticeable peak shown in Figure 9b is produced as an outcome of illuminating the change in the pipe specimen due to the sawcut. The result shows that Time Reversal change focusing is effective at identifying defects in the lateral direction of a pipe.

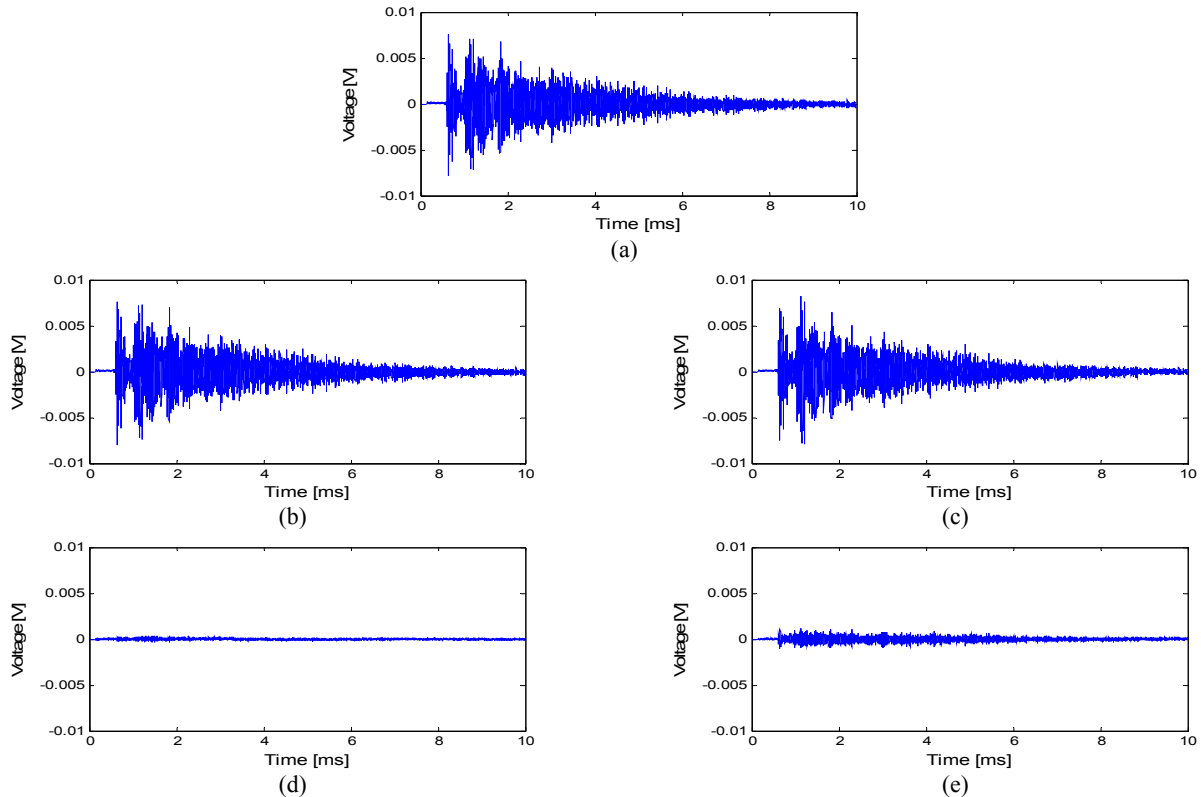


Figure 8. (a) Background clutter, (b) received signal before a lateral defect is induced, (c) received signal after a lateral defect is induced, (d) difference of (a) and (b), and (e) difference of (a) and (c).

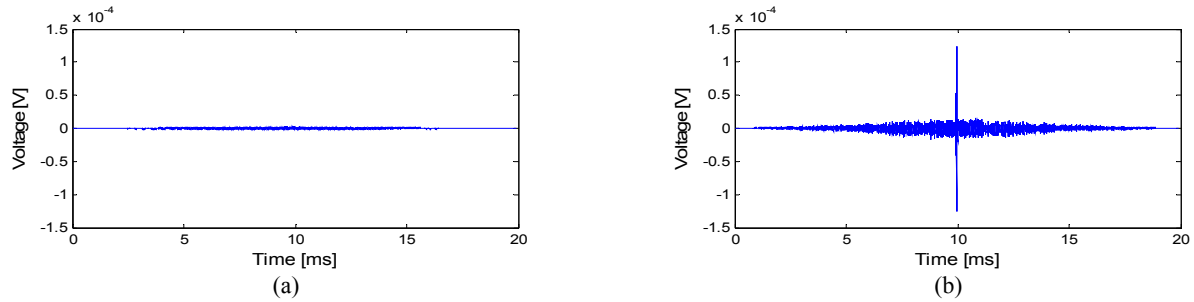


Figure 9. Time Reversal change focusing (a) before and (b) after a lateral defect is induced.

4.5 Pipe with a longitudinal defect

This experiment was conducted on a pipe specimen with length 1730 mm, outside diameter 74 mm and wall thickness 5 mm. A pair of PZT wafer transmitter and receiver was mounted 1000 mm apart on the pipe. Each wafer was 12 mm long and 6 mm wide. The input signal at the transmitter was a 200 kHz sinc pulse. A longitudinal notch, 220 mm long, 3 mm wide and 1 mm deep, was grinded into the pipe 450 mm from the transmitter.

After Time Reversal change focusing is applied, an evident peak is observed at the center of the plot shown in Figure 10b, as an indication of the change in the pipe caused by the longitudinal defect. The increase of the maximum amplitude is nearly 192 times or 45.7 dB, from 0.0146 mV to 2.8 mV (see Figure 10). The result shows that Time Reversal change focusing can effectively recognize defects in the longitudinal direction of a pipe. This observation is consistent with our expectation of scattering of pipe waves by such longitudinal defects.

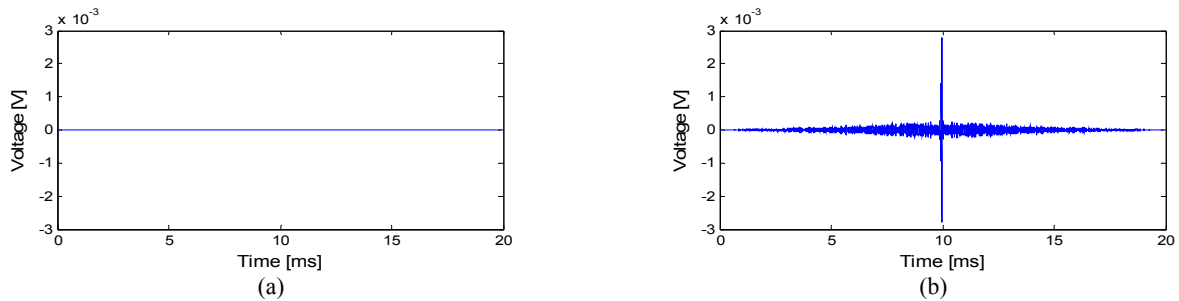


Figure 10. Time Reversal change focusing (a) before and (b) after a longitudinal defect is induced.

4.6 Pipe with a corrosion-like defect

A similar experiment was performed on a specimen with length 1730 mm, outside diameter 74 mm and wall thickness 5 mm, except for a corrosion-like defect over a small area on the surface of the pipe. The dent was 1 mm deep, with major axes 20 mm and minor axes 15 mm. A PZT wafer transmitter and a receiver were mounted 1000 mm apart on the pipe, 12 mm in length and 6 mm in width. The distance between the dent and the PZT transmitter was 300 mm. A sinc pulse center at 200 kHz was chosen as the excitation signal.

Figure 11 shows that Time Reversal change focusing can illuminate the corrosion-like defect by presenting a distinguishable peak in the received signal. The amplitude of the peak is about 14 times or 23.1 dB higher than the one before the dent is created, from 0.0425 mV to 0.6093 mV. Therefore, Time Reversal change focusing is also effective at identifying small corrosion-like defects in a pipe. This observation is consistent with our expectation of scattering of pipe waves by such corrosion-like defects.

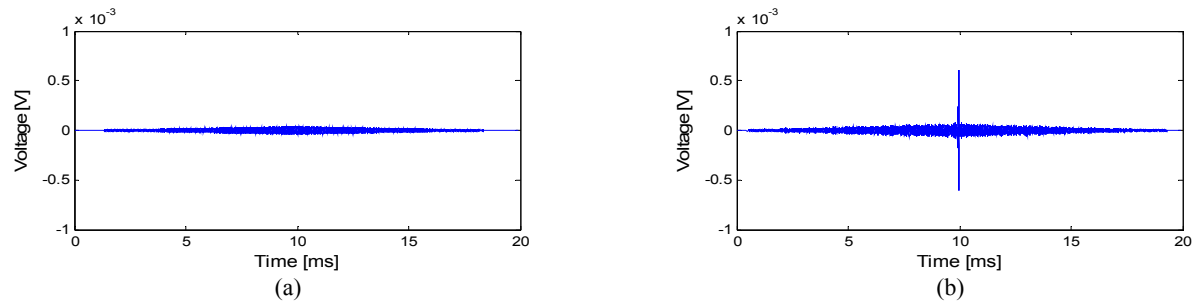


Figure 11. Time Reversal change focusing (a) before and (b) after a corrosion-like defect is induced.

Table 2. Experimental results of Time Reversal focusing of guided waves.

Exp. No	Pipe	Peak Level			Plots
		Received Signal	Time Reversal Focused Signal	Difference	
1	Simple pipe	41.0 mV	103.9 mV	8.1 dB	Figure 2
2	Pipe with welded butt joint	18.2 mV	37.2 mV	6.2 dB	Figure 3
3	Simple pipe with internal pressure	23.2 mV	33.7 mV	3.3 dB	Figure 7

Table 3. Experimental results of Time Reversal change focusing.

Exp. No	Defect Type	Peak Level after Time Reversal Change Focusing			Plots
		Before Defect Induced	After Defect Induced	Difference	
4	Lateral	0.0037 mV	0.1243 mV	30.6 dB	Figure 9
5	Longitudinal	0.0146 mV	2.8 mV	45.7 dB	Figure 10
6	Corrosion-like	0.0425 mV	0.6093 mV	23.1 dB	Figure 11

5. CONCLUSIONS

Time Reversal focusing has been shown to compensate for multiple modes and dispersion in pipe environment, resulting in an enhanced signal-to-noise ratio and effective change detection by presenting a distinguishable peak. This technique has been effectively demonstrated in six laboratory circumstances, providing with comprehensive and promising results on guided wave focusing in a pipe with/without welded joint, with/without internal pressure, and detection of three different defects: lateral, longitudinal and corrosion-like. The focusing feature allows Time Reversal to benefit long-distance and low-power pipeline monitoring, and also shows enormous prospective for Structural Health Monitoring and Nondestructive Evaluation applications in other infrastructures. It is noted that Time Reversal change focusing leads to different amplification factors of the received peak levels among various types of defects with different sizes. This phenomenon reflects Time Reversal's potential as a metric for evaluating the magnitude of damage in the pipe, which is envisioned as a part of our future work. Another challenging research topic would be how to distinguish and classify "changes" caused by different damage types as well as some operational and environmental variations.

ACKNOWLEDGMENTS

National Energy Technology Laboratory (NETL) is the funding source for this effort with Cost Share being provided by Carnegie Mellon University (CMU). Concurrent Technologies Corporation (CTC) is funded under a cooperative agreement with NETL. CMU is funded under a Subcontract Agreement with CTC. Joel Harley and Nicholas O'Donoghue are supported by National Defense Science and Engineering Graduate Fellowships, sponsored by the Office of Naval Research and the Army Research Office, respectively.

REFERENCES

- [1] Demma, A., Cawley, P., Lowe, M., and Roosenbrand, A.G., "The reflection of the fundamental torsional mode from cracks and notches in pipes," *The Journal of the Acoustical Society of America* 114 (2), 611-625 (2003).
- [2] Lowe, M.J.S., Alleyne, D.N., and Cawley, P., "Defect detection in pipes using guided waves," *Ultrasonics* 36(1-5), 147-154 (1998).
- [3] Rose, J.L., [Ultrasonic Waves in Solid Media], Cambridge University Press, Cambridge, (1999).
- [4] Shull, P.J., [Nondestructive evaluation: theory, techniques, and applications], Marcel Dekker, Inc., New York, (2002).
- [5] Cawley, P., "Practical Long Range Guided Wave Inspection—Managing Complexity," in *AIP Conference Proceedings* 657, 22-40 (2003).
- [6] Lowe, M.J.S., and Cawley, P., "Long Range Guided Wave Inspection Usage—Current Commercial Capabilities and Research Directions." Department of Mechanical Engineering, Imperial College London, London, (2006).
- [7] Fink, M., "Time reversal of ultrasonic fields—Part I: Basic principles," *IEEE Trans. Ultrason. Ferroelectr. Freq. Control* 39(5), 555-566 (1992).
- [8] Prada, C., and Fink, M., "Separation of interfering acoustic scattered signals using the invariants of the time-reversal operator. Application to Lamb waves characterization," *The Journal of the Acoustical Society of America* 104, 801-807 (1998).
- [9] Ing, R.K., and Fink, M., "Time-reversed Lamb waves," *IEEE Transactions on Ultrasonics, Ferroelectrics, and Frequency Control* 45(4), 1032-1043 (1998).
- [10] Sohn, H., Park, H.W., Law, K.H., and Farrar, C.R., "Damage Detection in Composite Plates by Using an Enhanced Time Reversal Method," *Journal of Aerospace Engineering* 20(3), 141-151 (2007).
- [11] Park, H.W., Sohn, H., Law, K.H., and Farrar, C.R., "Time reversal active sensing for health monitoring of a composite plate," *Journal of Sound and Vibration* 302(1-2), 50-66 (2007).
- [12] Nunez, I., and Negreira, C., "Efficiency parameters in time reversal acoustics: Applications to dispersive media and multimode wave propagation," *The Journal of the Acoustical Society of America* 117(3), 1202-1209 (2005).
- [13] Moura, J.M.F., and Jin, Y., "Detection by time reversal: single antenna," *IEEE Transactions on Signal processing* 55(1), 187-201(2007).
- [14] Jin, Y., and Moura, J.M.F., "Time-Reversal Detection Using Antenna Arrays," *IEEE Transactions on Signal Processing* 57(4), 1396-1414 (2009).
- [15] Li, J., and Rose, J.L., "Excitation and propagation of non-axisymmetric guided waves in a hollow cylinder," *The Journal of the Acoustical Society of America* 109, 457-464 (2001).
- [16] Seco, F., Martín, J.M., Jiménez, A., Pons, J.L., Calderón, L., and Ceres, R., "PCDISP: a tool for the simulation of wave propagation in cylindrical waveguides," in *Proceedings of the 9th International Congress on Sound and Vibration*, 23-29(2002).
- [17] O'Donoghue, N., Harley, J., Moura, J.M.F., Jin, Y., Oppenheim, I.J., Ying, Y., States, J., Garrett, J.H., and Soibelman, L., "Single Antenna Time Reversal of Guided Waves in Pipelines," in *Proceedings of Meetings on Acoustics* 6(1), 065001-11 (2009).
- [18] Harley, J., O'Donoghue, N., States, J., Ying, Y., Garrett, J.H., Jin, Y., Moura, J.M.F., Oppenheim, I.J., and Soibelman, L., "Focusing of Ultrasonic Waves in Cylindrical Shells using Time Reversal," in *Proceedings of the 7th International Workshop on Structural Health Monitoring*, (2009).
- [19] Prada, C., Manneville, S., Spoliansky, D., and Fink, M., "Decomposition of the time reversal operator: Detection and selective focusing on two scatterers," *The Journal of the Acoustical Society of America* 99(4), 2067-2076 (1996).